Basic

European Journal of Immunology

Adaptive immunity

Research Article

Flow cytometry-based high-throughput RNAi screening for miRNAs regulating MHC class II HLA-DR surface expression

Maja Houseman[#1,2], *Melody Ying-Yu Huang*[#1,2,3], *Markus Huber*[1,2], *Matthias Staiger*[1,2], *Lan Zhang*[1,2], *Anneliese Hoffmann*[1,2], *Christoph Lippuner*[1,2] *and Frank Stüber*[1,2]

[1] Department of Anaesthesiology and Pain Medicine, Inselspital, Bern University Hospital, University of Bern, Bern, Switzerland
[2] Department for BioMedical Research, University of Bern, Bern, Switzerland
[3] Department of Health Sciences and Technology, Swiss Federal Institute of Technology (ETH) Zürich, Zürich, Switzerland

HLA-DR isotype is a MHC-II cell-surface receptor found on APCs and plays a key role in initiating immune responses. In severely immunocompromised patients with conditions like sepsis, the number of HLA-DR molecules expressed on leukocytes is considered to correlate with infectious complications and patients' probability of survival. The underlying regulatory mechanisms of HLA-DR expression remain largely unknown. One probable path to regulation is through microRNAs (miRNAs), which have been implicated as regulatory elements of both innate and adaptive immune system development and function. In our study, flow cytometry-based high-throughput miRNA screening was performed in a stable HLA-DR-expressing human melanoma cell line, MelJuSo, for either up- or downregulating miRNAs of the surface HLA-DR expression. By the end of the screening, the top ten upregulators and top five downregulators were identified, and both the HLA-DR protein and mRNA regulations were further verified and validated. In-silico approaches were applied for functional miRNA-mRNA interaction prediction. The potential underlying gene regulations of different miRNAs were proposed. Our results promote the study of miRNA-mediated HLA-DR regulation under both physiological and pathological conditions, and may pave the way for potential clinical applications.

Keywords: antigen-presenting cells (APCs) · human leukocyte antigen (HLA) · MHC class II · microRNA (miRNA) · transfection

Additional supporting information may be found online in the Supporting Information section at the end of the article.

Correspondence: Dr. Melody Ying-Yu Huang and Frank Stüber
e-mail: melody.yingyu.huang@gmail.com; frank.stueber@insel.ch

[#] Maja Houseman and Melody Ying-Yu Huang are the co-first authors.

Introduction

MHC-I/II molecules are important proteins that play a critical role in the immune response. HLA-DR isotype (HLA-DR) is an MHC-II cell-surface receptor typically found on professional APCs such as monocytes or DCs. The primary function of HLA-DR is to display processed antigens on APCs to appropriate immune cells, such as cluster of differentiation 4 (CD4)+ T cells; [1] however, activation of HLA-DR expression on CD8+ cytotoxic T cells has also been associated with autoimmune diseases, HIV, and breast cancer [2–4]. Clinically, decreased HLA-DR surface expression levels on CD14+ monocytes have been shown to correlate with higher mortality in sepsis, or to demonstrate a higher risk of acquiring severe nosocomial infections [5].

Besides decreased HLA-DR surface expression, the other frequently used clinical indicator of monocytic immune incapacity associated with immunosuppression is decreased levels of ex-vivo LPS-induced TNF-alpha production. However, with the latter not being able to reliably distinguish among disease severity levels, monocytic HLA-DR surface expression may prove to be a more accurate predictor of mortality and/or acquisition of nosocomial infections in critically ill patients from surgical or medical intensive care units [6–11]. Recently, monocytic HLA-DR surface expression was used as one critical immunological parameter in monitoring severe cases of coronavirus disease 2019 [12–15].

During biological processes, protein expression can be regulated by several mechanisms, one of which is RNA interference (RNAi), the interaction of siRNA, or micro RNA (miRNA) with mRNA. A high-throughput RNAi screening detecting HLA-DR surface expression may pave the way for the development of new therapeutic approaches and for identifying novel peripheral blood biomarkers of severe infections.

In a previous study, a systematic genome-wide flow cytometry (FCM)-based siRNA screening targeting MHC-II expression and peptide loading revealed factors and underlying transcriptional networks and transport pathways of MHC-II regulation that may be linked to infection and autoimmunity [16]. For instance, TGF-β signaling may be involved in MHC-II transcriptional regulation via RMND5B and SMADs. Further, a pathway of the GTPase ARL14/ARF7 and actin-based motor myosin 1E has been linked to the MHC-II transport controls in DCs. In contrast to siRNA, little has been reported with regard to miRNA's involvement in MHC-II regulation. siRNA and miRNA, which differ mainly in their mRNA target-binding specificity, possess mechanisms of action and clinical applications which are not yet distinct.

In the current study, we used a stable MHC-II-expressing human melanoma cell line, MelJuSo [16, 17], to perform FCM-based high-throughput miRNA screening for the first time. The aim was to identify miRNAs with either up- or downregulating activity of surface HLA-DR expression. To ensure the suitability and high quality of our screening assay, we computed the screening window coefficient *Z'*-factor for the assay quality assessment [18]. Moreover, we applied a statistical method that is intended specifically for cell-based RNAi screening analysis, which takes into account the considerable between-plate variation found in the cytometry methods [19].

According to the calculated rank order, we identified ten HLA-DR upregulating and five downregulating miRNA candidates from approximately 2000 human miRNA compounds stored in the miRIDIAN miRNA mimic library. By the end of the RNAi screening, we had successfully verified the miRNA regulation of surface HLA-DR expression with separate FCM assays. Furthermore, we validated the RNAi effect on the *HLA-DRA* mRNA expression using quantitative real-time PCR (*qPCR*) and compared the results with those of the protein regulation.

Results

Large-scale miRNA screen

Instead of using APCs, we chose the human melanoma cell line MelJuSo, which has stable constitutive HLA-DR surface expression but lacks many other immune-specific gene expressions. This was used to perform a large-scale, high-throughput FCM-based screening for miRNA candidates regulating the HLA-DR surface expression. With this approach, we were better able to focus on the miRNA-regulated HLA-DR pathways by avoiding certain indirect RNAi-modulated HLA-DR expression alterations via other immune factors. TLRs, for example, are known to interact with antisense and siRNA [16, 20, 21].

A total of approximately 2000 miRNA mimics from the miRIDIAN miRNA mimic library (see "Methods") were individually transfected into MelJuSo cells on 96-well plates. The siRNA Hs_CIITA_2, targeting the MHC-II transactivator CIITA, known to downregulate CIITA and, thus, HLA-DR, was employed in our transfection assay as the positive control [22, 23]. In addition, two *Caenorhabdits elegans* miRNAs–cel-miR-67 and cel-miR-239b–which have no known target sequence in human cells, were included as negative controls.

To visualize the regulatory effect of miRNA on HLA-DR surface expression in MelJuSo cells, a monoclonal mouse anti-human HLA-DR antibody detecting peptide-loaded MHC-II/HLA-DR was used for cell-surface staining prior to the FCM analysis [24]. All experiments were performed three times. The overall cell viability of our transfection assay was estimated to be 88%, which was calculated using the fixable viability dye eFluor 506 (eBioscience). Moreover, the miRNA transfection efficiency in MelJuSo cells was estimated to be more than 90% according to the Dy547-labelled miRNA hairpin inhibitor transfection control.

First, we applied the FCM analysis and computed the MFI of each individual well. Next, to ensure and validate the quality of the RNAi assays, we adapted a statistical method and computed the Z'-factor, a popular parameter for HTS experiments (see "Methods") [18, 19]. Figure 1 shows box plots of MFIs of the three experimental sets of the FCM data, grouped by plate A and B (A1-A25, B1-B25) and sample type (sample, positive and negative controls). In both A and B experiments, the assignment of miRNAs to plates was quasi randomized; however, as shown in Figure 1A

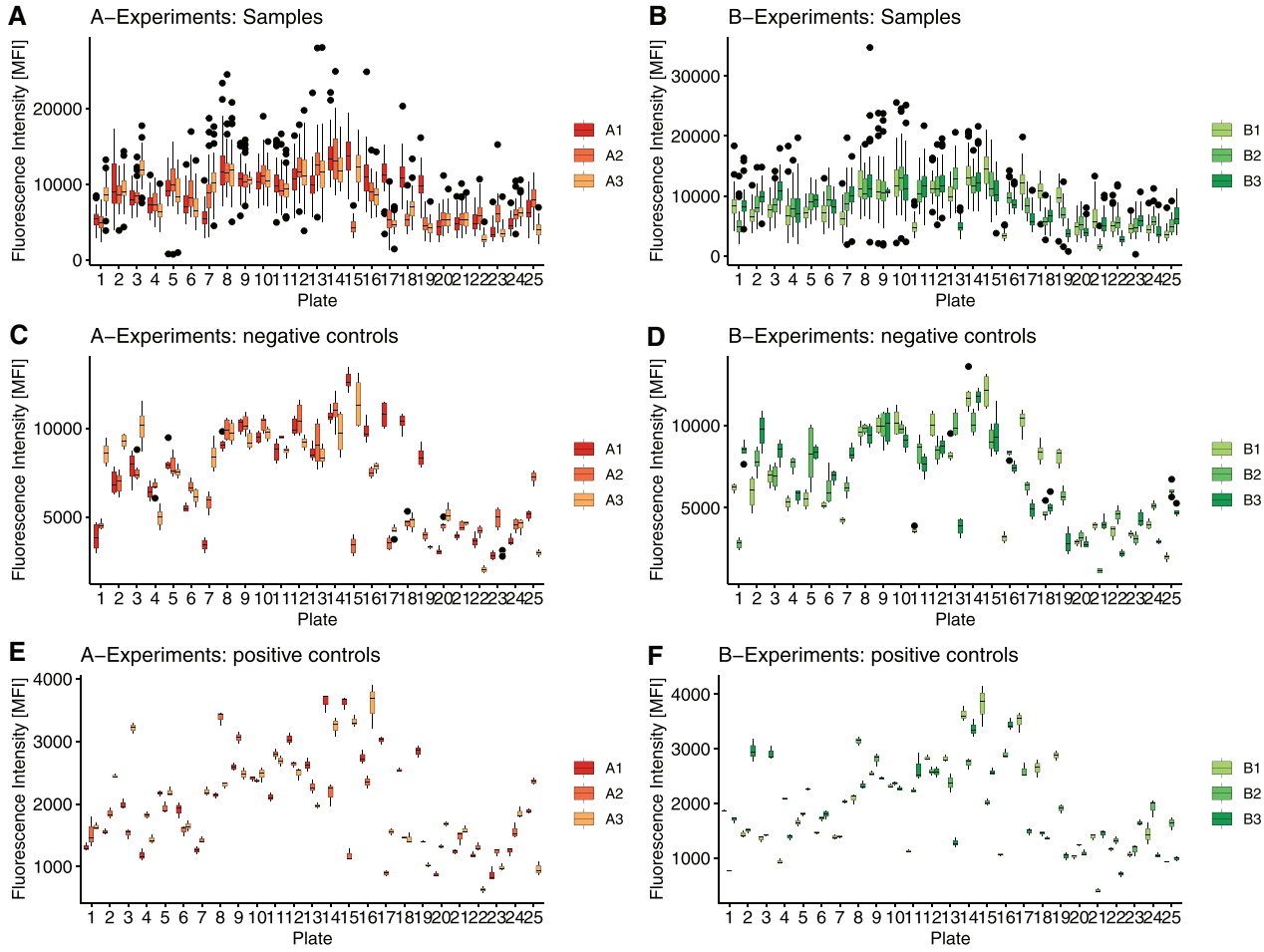

Figure 1. Flow cytometry (FCM) analysis of HLA-DR surface expression in a large-scale miRNA screen. Box-and-whiskers plots are used to illustrate the median values, upper and lower quartiles as well as outliers of Median Fluorescence Intensity (MFI) of the three independent experiments (N = 3) of the FCM data, grouped by plate A and B (A1-A25, B1-B25) and sample types: (A) miRNA samples, (B) positive controls, and (C) negative controls.

and 1B, the absolute MFI values varied across plates. In addition, a similar plate-specific MFI pattern was observed among samples (Fig. 1A-B) and controls (Fig. 1C and D for negative controls, 1E-F for positive controls) throughout the experiments.

Thus, to achieve a more biologically significant measure of the experimental effect, we conducted plate-based MFI data normalization and transformation and computed the z-scores of all the samples (see "Methods") [19]. The normalized sample values are shown in Supporting information Figure S1. An overview of the computed z-scores of all experiments can be seen in Figure 2. The means of z-scores from three independent experimental replicates were computed for all tested miRNA molecules. Based on the results, we generated a list of top-scoring miRNAs (for both positive and negative scores) that can be selected as candidate *HLA-DR* miRNA regulators. Specifically, we defined z-score +4 and -3 as the thresholds for top up- and downregulating miRNAs, respectively (see "Methods"). As a result, ten upregulating and five downregulating miRNAs were identified for surface HLA-DR expression regulators. These are listed in Tables 1 and 2. We applied a bootstrap sensitivity analysis to further validate our identified top results. Analysis of the results confirms the Z-scoring method as a robust predictor of the upregulating (Fig. 3A) and downregulating (Fig. 3B) molecules.

Verification and validation of the miRNA modulation of HLA-DR expression

To verify the regulating effects on the surface HLA-DR expression during the RNAi screening, we randomly picked five out of the top ten upregulating miRNAs and all five of the downregulating miRNAs. These were used to carry out an independent cell transfection assay in MelJuSo cells. The FCM result is depicted in Figure 4. All the tested miRNA molecules confirmed similar up- and downregulating protein regulatory effects, as revealed in the screening assays. These further verified the FCM-based HTP RNAi screening method.

Next, we aimed to validate the miRNA regulating effects of all the up- and downregulating hits on the *HLA-DR*A transcript level [25]. For this, we collected the transfected MelJuSo cells

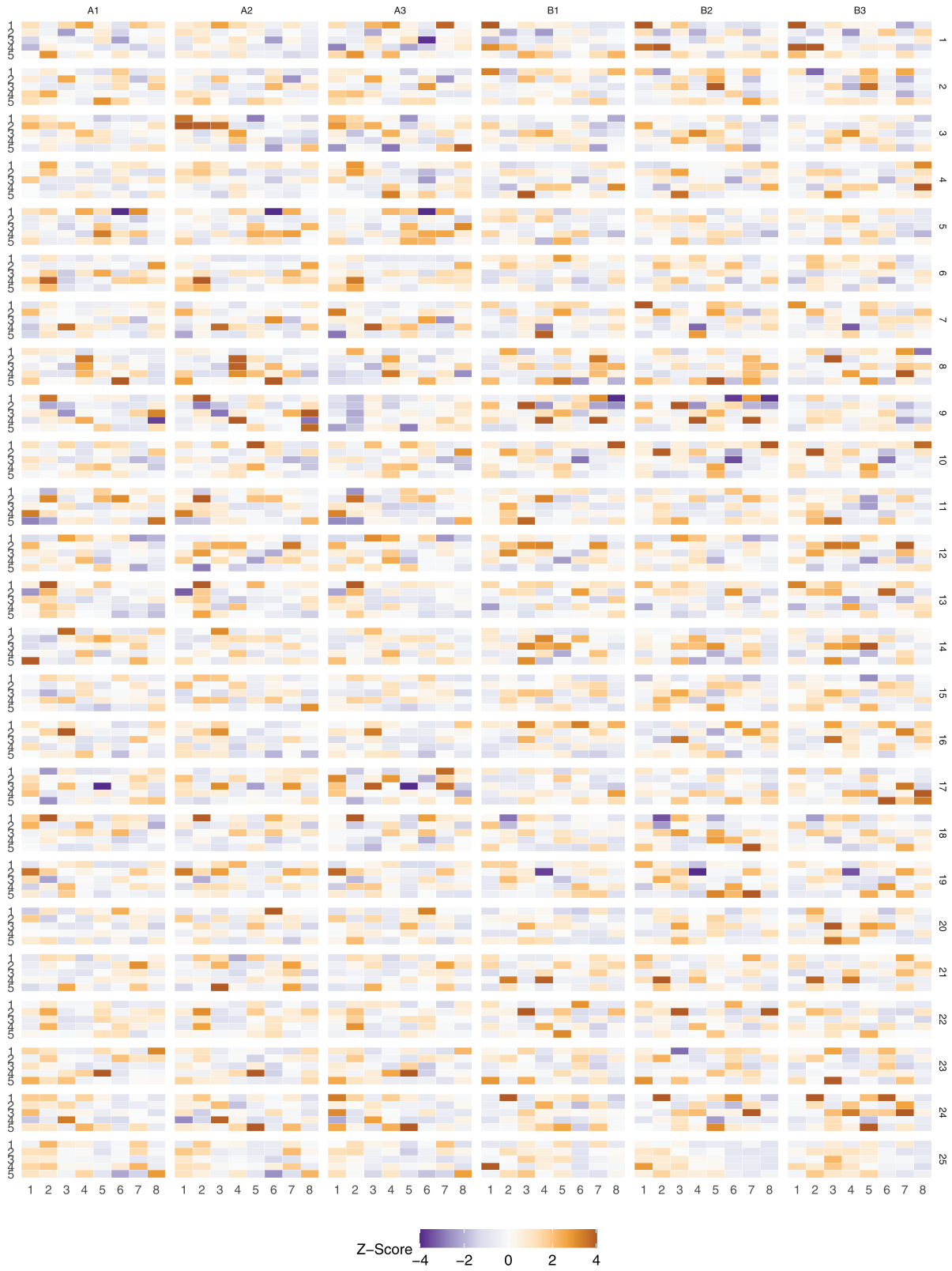

Figure 2. Overview of the computed sample z-scores of all three experiments. Plate-based data normalization and transformation of Median Fluorescence Intensity (MFI) measurements was performed, and the MFI data were computed into z-scores (see "Methods"). Robust z-scores values for each plate in all three independent experiments (A1, A2, A3 and B1, B2, B3) can been seen.

Table 1. Median Fluorescence Intensity (MFI) values and corresponding z-scores—both individually and the mean across three repeats—are shown for the miRNA considered a hit with z-scores above the threshold of 4

z-score > 4

Plate	Col	Row	Experiment	Mature name	Fluorescence (MFI)	MFI normalized	z-score	z-score (mean)
1	3	1	B1	hsa-miR-214-3p	18372	2.18	5.87	5.86
1	3	1	B2	hsa-miR-214-3p	13327	2.75	6.03	5.86
1	3	1	B3	hsa-miR-214-3p	16344	2.01	5.68	5.86
8	8	5	A1	hsa-miR-513a-3p	23371	2.01	4.23	4.75
8	8	5	A2	hsa-miR-513a-3p	24508	2.14	7.67	4.75
8	8	5	A3	hsa-miR-513a-3p	17988	1.51	2.35	4.75
8	9	4	B1	hsa-let-7f-2-3p	15455	1.38	2.11	4.06
8	9	4	B2	hsa-let-7f-2-3p	14449	1.40	2.06	4.06
8	9	4	B3	hsa-let-7f-2-3p	34746	3.12	8.01	4.06
10	10	1	B1	hsa-miR-205-3p	25580	2.17	4.33	4.04
10	10	1	B2	hsa-miR-205-3p	24566	1.90	4.09	4.04
10	10	1	B3	hsa-miR-205-3p	22184	1.99	3.70	4.04
13	4	1	A1	hsa-miR-3115	22079	2.23	7.20	6.78
13	4	1	A2	hsa-miR-3115	28005	2.24	7.50	6.78
13	4	1	A3	hsa-miR-3115	28072	2.42	5.65	6.78
18	4	1	A1	hsa-miR-4487	20327	1.88	4.81	4.41
18	4	1	A2	hsa-miR-4487	9862	1.88	3.94	4.41
18	4	1	A3	hsa-miR-4487	13357	1.91	4.47	4.41
21	4	4	B1	hsa-miR-4753-5p	12381	2.14	3.40	4.45
21	4	4	B2	hsa-miR-4753-5p	5039	3.39	6.18	4.45
21	4	4	B3	hsa-miR-4753-5p	10156	2.03	3.77	4.45
23	7	4	A1	hsa-miR-5003-3p	7663	2.30	5.44	5.97
23	7	4	A2	hsa-miR-5003-3p	15241	2.51	5.51	5.97
23	7	4	A3	hsa-miR-5003-3p	8355	2.38	6.95	5.97
24	4	1	B1	hsa-miR-5693	8834	2.02	4.63	4.40
24	4	1	B2	hsa-miR-5693	9197	1.61	4.25	4.40
24	4	1	B3	hsa-miR-5693	6926	1.91	4.33	4.40
24	9	3	B1	hsa-miR-5581-5p	4614	1.06	0.26	4.49
24	9	3	B2	hsa-miR-5581-5p	11273	1.97	6.80	4.49
24	9	3	B3	hsa-miR-5581-5p	8524	2.36	6.42	4.49

48 h after transfection and performed a real-time *qPCR* analysis. Figure 5 shows the *HLA-DRA* mRNA expression after the miRNA transfection. Interestingly, the upregulating effects of the miRNA hits on the mRNA level were generally not as pronounced, compared to the protein expression. On the other hand, the downregulating effects of the miRNA hits on the mRNA level better reflected the protein expression regulation, although the treatment with hsa-miR-1202 led to elevated *HLA-DRA* mRNA expression 48 h after transfection, followed by decreased surface HLA-DR expression 72 h after transfection.

Finally, we also examined the potential miRNA-regulating effects of all the up- and downregulating hits on both *HLA-DRB1* and *CIITA* transcript levels. Surprisingly, despite sharing comparable gene-regulating effects of both negative and positive RNAi controls on the *HLA-DRA* mRNA expression, no downregulating effect on *HLA-DRB1* mRNA expression was detected among the five miRNA hits. On the other hand, the upregulating effects seemed to remain to a certain degree such as they were seen with hsa-miR-214-3p, hsa-miR-4487, and hsa-miR-5003-3p (Supporting information Fig. S2). As for the *CIITA*, general up- and downmRNA regulations were not obvious; however, individual upregulating trends of a few miRNA molecules on *CIITA* expression could be observed (e.g., hsa-miR-214-3p, hsa-miR-3115, hsa-miR-4487, and hsa-miR-5003-3p), similar to the effects seen in both *HLA-DRA* and *HLA-DRB1* gene regulations (Supporting information Fig. S3). Taken together, the downregulating effects specifically seen on *HLA-DRA* may suggest a direct interaction between the miRNAs and the *HLA-DRA* mRNA. On the other hand, those miRNAs that show similar upregulating effects on all *HLA-DRA*, *HLA-DRB1*, and *CIITA* may have shared or overlapping underlying indirect gene regulation pathways.

Discussion

In this study, we performed FCM-based high-throughput miRNA screening with the aim of identifying miRNAs with either up- or downregulating effect on surface HLA-DR expression. By the end of the RNAi assay, we had successfully identified and validated 15 miRNA candidates that modulated *HLA-DRA* and/or surface

Table 2. Median Fluorescence Intensity (MFI) values and corresponding z-scores–both individually and the mean across three repeats–are shown for the miRNA considered a hit with z-scores below the threshold of −3

z-score < −3

Plate	Col	Row	Experiment	Mature name	Fluorescence (MFI)	MFI normalized	z-score	z-score (mean)
5	8	1	A1	hsa-miR-567	782	0.09	-6.52	-5.163333
5	8	1	A2	hsa-miR-567	737	0.07	-4.32	-5.163333
5	8	1	A3	hsa-miR-567	968	0.12	-4.65	-5.163333
7	6	4	B1	hsa-miR-151a-5p	2076	0.33	-2.72	-3.080000
7	6	4	B2	hsa-miR-151a-5p	1920	0.22	-3.17	-3.080000
7	6	4	B3	hsa-miR-151a-5p	2414	0.24	-3.35	-3.080000
10	8	3	B1	hsa-miR-1202	2181	0.19	-3.01	-3.160000
10	8	3	B2	hsa-miR-1202	2934	0.23	-3.53	-3.160000
10	8	3	B3	hsa-miR-1202	2368	0.21	-2.94	-3.160000
17	7	3	A1	hsa-miR-151b	3420	0.31	-4.00	-3.886667
17	7	3	A2	hsa-miR-151b	1322	0.25	-2.34	-3.886667
17	7	3	A3	hsa-miR-151b	1437	0.31	-5.32	-3.886667
19	6	2	B1	hsa-miR-3972	2452	0.25	-3.69	-3.983333
19	6	2	B2	hsa-miR-3972	1555	0.23	-4.84	-3.983333
19	6	2	B3	hsa-miR-3972	775	0.21	-3.42	-3.983333

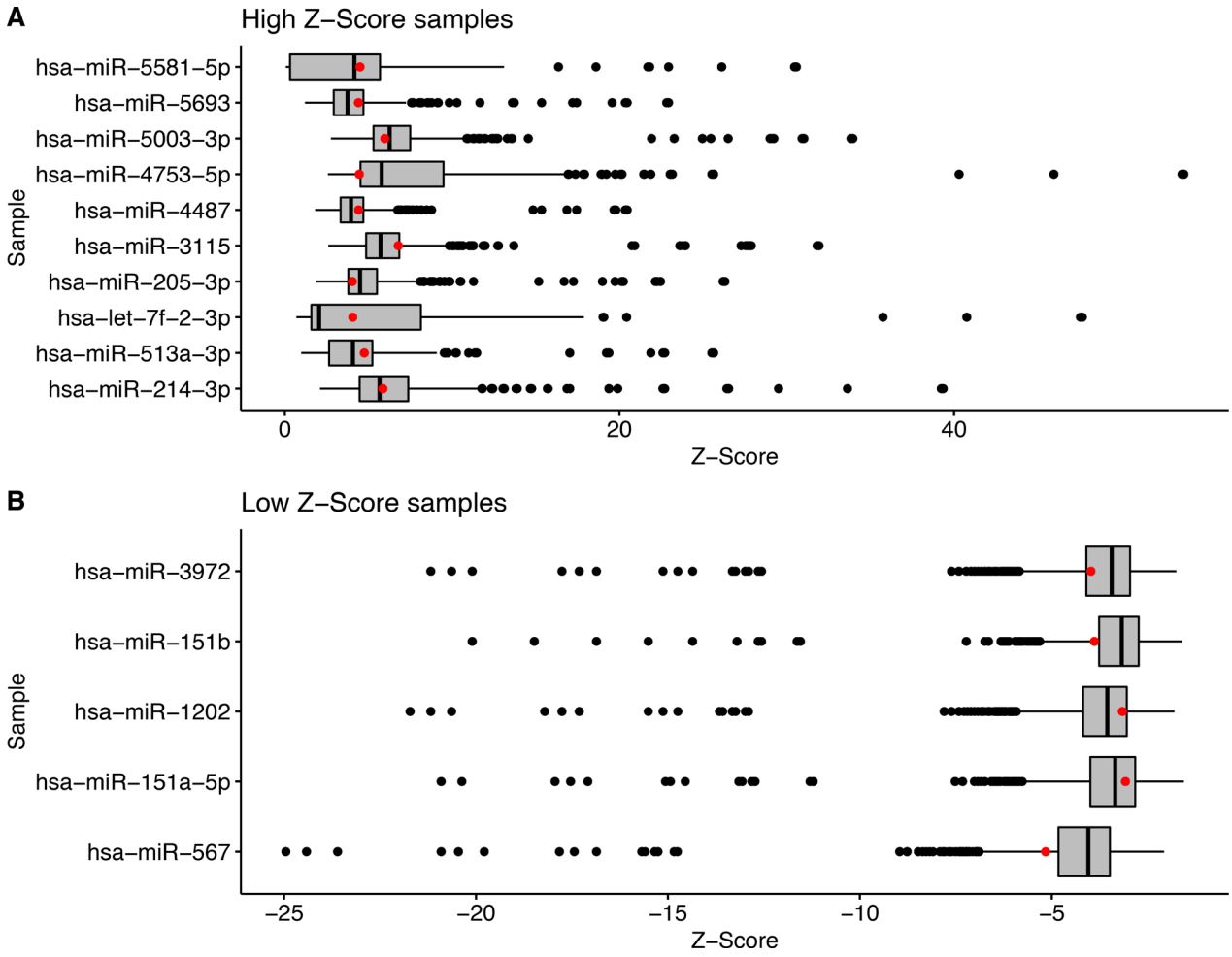

Figure 3. Sensitivity analysis of the selected top up- and downregulating miRNA molecules. Box-and-whiskers plots illustrating the median values, upper and lower quartiles, as well as outliers of z-scores of each (A) up- and (B) downregulating miRNA hits in the sensitivity analysis. The sensitivity analysis is based on a permutation approach (refer to Statistical Analysis) and examines how strongly the z-scores of each hit depends on the normalized Median Fluorescence Intensity (MFI) values of the corresponding plate.

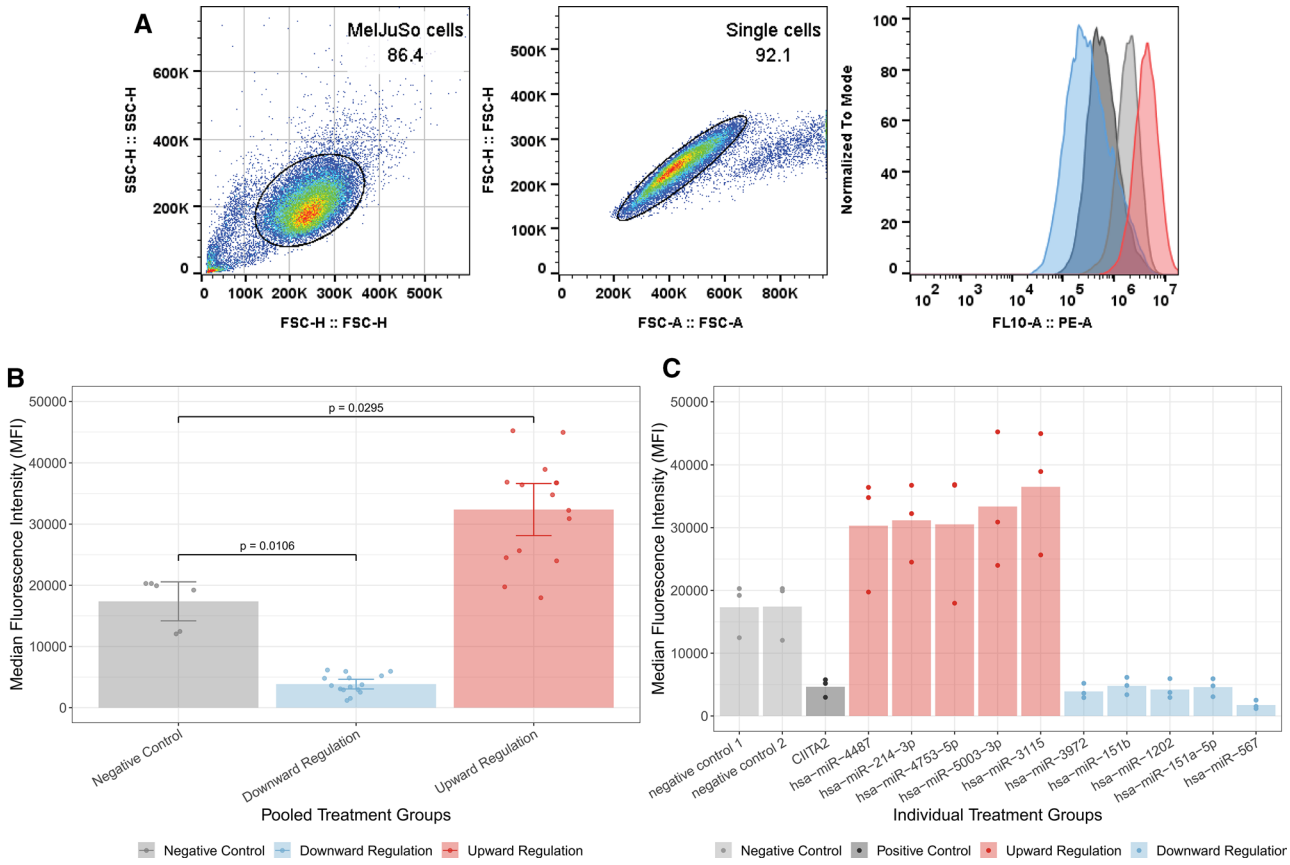

Figure 4. Regulating effect of ten selected miRNAs on HLA-DR surface expression. Flow cytometry was conducted to estimate HLA-DR surface expression 72 h after transfection in human cell line MelJuSo. (A) Representative dot plots gating MelJuSo population, single cells, and histogram of surface HLA-DR protein expression levels in gated MelJuSo single cells transfected with different small noncoding RNA molecules (light gray: negative control miRNA mimics, dark gray: positive control siRNA targeting CIITA, blue: downregulating miRNA, and red: upregulating miRNA). (B) Comparison of the Median Fluorescence Intensity (MFI) of surface HLA-DR among pooled treatments groups (gray: negative control miRNA mimics based on *C. elegans* sequences, blue: downregulating miRNAs, and red: upregulating miRNAs). Mean MFI values per group and associated 95% confidence intervals are shown. To perform group comparisons, a linear mixed-effect model with a fixed effect was used for treatment (three levels: negative control, down-, and upregulation) and a random slope was used for each experiment and each treatment (see "Methods"). MFI values were transformed using Ordered Quantile normalization to ensure a normally distributed outcome in the linear mixed-effect model. Estimated marginal means (EMMs) were employed to compute the contrasts of the two treatments and compare them with the negative control samples. No *p*-value adjustment for multiple comparisons was used, as the *p*-values were exploratory rather than confirmatory in this study. (C) Mean MFIs for verification samples. Colored dots represent individual samples from three independent experiments (N = 3).

HLA-DR expression in an APC-like human melanoma cell line, MelJuSo. In a previous study, large-scale genome-wide screening conducted by Paul and colleagues using several siRNA oligos to target each gene suggested that there are underlying genetic pathways for MHC-II antigen-presentation regulation [16]. Compared to siRNA, which is an exogenous ds RNA taken up by cells and targeting one specific gene, miRNA is a ss endogenous noncoding RNA that often targets multiple related genes belonging to the same cellular pathway or process, making it an excellent candidate as a drug target or diagnostic and biomarker tool, in addition to a therapeutic agent [26]. The RNAi process is mediated by a ribonucleoprotein called RNA-induced silencing complex (RISC). The miRNA-RISC complex recognizes and degrades, cleaves, or represses the complementary mRNA, resulting in one of the key translational gene-silencing processes [27–29]. Besides post-transcriptional regulation, miRNAs can also be involved in transcriptional gene silencing [30]. Moreover, an miRNA can interact with various target mRNAs, and conversely, an mRNA can be regulated by several miRNAs [31]. Finally, empirical evidence shows that miRNAs not only induce gene silencing but may also enhance translation by stabilizing their target mRNAs [32].

According to our *qPCR* validation results, all but one (hsa-miR-1202) of the surface HLA-DR downregulating miRNAs also showed a downregulating effect on *HLA-DRA* mRNA expression. One plausible explanation is that hsa-miR-1202 may suppress HLA-DR expression via the translational (i.e., post-transcriptional) gene silencing process, while the other downregulators may modulate *HLA-DRA* expression through transcriptional gene silencing, or more likely, through GW182-mediated mRNA degradation [29] or other indirect molecular pathways. As for the upregulating molecules, among those which

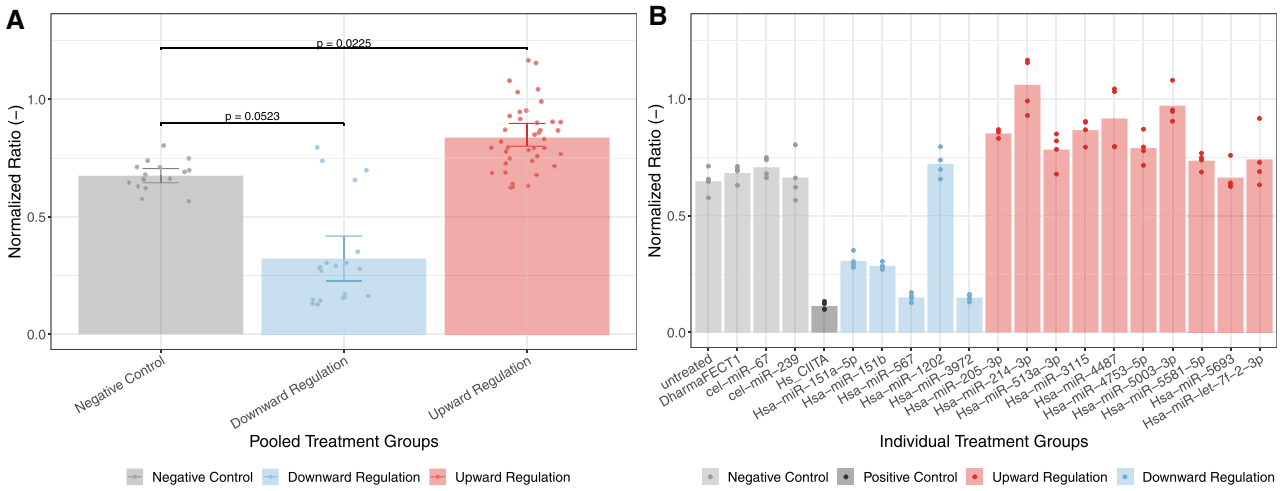

Figure 5. Regulating effect of all selected miRNAs on *HLA-DRA* mRNA expression. Real-time quantitative PCR (*q*PCR) was performed to estimate *HLA-DRA* transcript expression 48 h after transfection in human cell line MelJuSo. Two housekeeping genes glyceraldehyde-3-phosphate dehydrogenase (*GAPDH*) and hypoxanthine phosphoribosyl-transferase 1 (*HPRT1*) were used as reference genes. The relative quantification is calibrator normalized with efficiency correction and the result of the data analysis is expressed as a normalized ratio. (A) Comparison of the normalized ratio of *HLA-DRA* among pooled treatments groups (gray: negative controls of untreated cells, cells treated with transfection reagent only, and cells treated with two miRNA mimics based on *C. elegans* sequences; blue: downregulating miRNAs; and red: upregulating miRNAs). Mean normalized ratios per group and associated 95% confidence intervals are shown. To perform group comparisons, a linear mixed-effect model with a fixed effect was used for treatment (three levels: negative control, down-, and upregulation) and a random slope was used for each experiment and each treatment (see "Methods"). The normalized ratio was transformed using an Ordered Quantile normalization to ensure a normally distributed outcome in the linear mixed-effect model. Estimated marginal means (EMMs) were employed to compute the contrasts of the two treatments and compare them with the negative control samples. No *p*-value adjustment for multiple comparisons was used, as the *p*-values were exploratory rather than confirmatory in this study. (B) The normalized ratios for verification samples. Colored dots represent individual samples from four independent experiments (N = 4).

show an upregulating effect on both HLA-DR surface protein and *HLA-DRA* (and *HLA-DRB1*) mRNA levels, indirect transcriptional regulation may be involved (e.g., hsa-miR-205-3p, hsa-miR-214-3p, hsa-miR-3115, hsa-miR-4487, and hsa-miR-5003-3p). On the other hand, for those surface HLA-DR upregulators that did not show a clear regulating effect on the mRNA level, the regulation could be achieved by altering the transport and/or cellular localization of HLA-DR molecules [16], or the modulation may be performed by stabilizing the mRNA and, thus, enhancing HLA-DR translation (e.g., hsa-miR-5581-5p, hsa-miR-5693, and hsa-miR-let-7f-2-3p).

To further validate the potential miRNA/mRNA target interactions, we adopted in-silico approaches by using both the miRDB and TargetScan databases for target prediction of our candidate miRNA modulators. These database engines apply algorithms that are based on general information about interactions between the two RNA oligo sequences (e.g., seed sites and conservation) [33–35]. The search results, defined by an individual score, have predicted interaction of the miRNAs hsa-miR-567, hsa-miR-1202, and hsa-miR-3972 with *HLA-DRA* mRNA at a higher level of confidence in both databases (Supporting information Tables S1 and S2). However, one should note that up to now, the level of verified physiological relevance of such predicted interactions is rather minor [36]. Nevertheless, by incorporating new gene sequencing technologies and taking advantage of the increasing empirical data available, improvements in predictive power are likely with time [37]. Future research is likely to include experimental validation of the proposed functional miRNA/mRNA target pairs that fulfill well-defined experimental criteria, such as miRNA or mRNA coexpression, interaction of miRNA with a specific binding site, and miRNA effects on target protein expression and on biological function.

Clinically, HLA-DR surface expression on circulating monocytes has been adopted as a reliable indicator of clinical infection [11]. The number of HLA-DR surface molecules per monocyte decreases after a surgery [38] and remains at a downregulated level for 48 h after operation [39]. Surgical trauma is often linked to postoperative immune dysfunction, with postoperative sepsis being an especially critical condition. Specifically, major and extended surgery leads to significantly reduced expression of HLA-DR on peripheral blood monocytes [40], which has been associated with increased mortality in various clinical studies [41–43]. The pathological mechanism responsible for the suppressed immune response, for example, in post-traumatically acquired sepsis, remains unclear. A better understanding of the molecular regulation of HLA-DR will shed some light on immunoregulatory molecules in immunocompromised patients.

In recent years, microRNAs have gained recognition in clinical applications such as disease biomarkers or therapeutic interventions [44, 45]. Much effort has been devoted to identifying miRNAs for human cancer diagnosis and therapy [46–48]. In perioperative and critical care medicine, on the other hand, circulating miRNAs are emerging as a novel and promising diagnostic approach to treating sepsis [49–51]. However, new evidence is

needed to link the underlying MHC-II dysregulation to the associated miRNA molecules [52–54].

In the quest for innate immunomodulatory miRNAs for HLA-DR regulation, a greater high-throughput level of flow cytometric screening would be helpful. While the human MelJuSo cell line has provided an excellent in vitro platform for conducting such a screening, owing to its stable constitutive HLA-DR expression, the translatability of the screening outcome to preclinical immunology ultimately relies on comparable experimental findings using immune cell lines and/or primary leukocytes. Hence, we have tested the selected miRNA molecules using different human monocytic cell lines, and the preliminary results indeed confirmed a similar trend of regulatory effects on HLA-DR expression (unpublished data). Nevertheless, individual miRNA candidates identified through the RNAi screening may evoke different regulatory effects in primary cells, especially in an ex vivo whole-blood culture system that more closely resembles physiological conditions. Thus, follow-up studies using primary cells to scrutinize specific miRNA-regulating effects on HLA-DR regulation will be indispensable.

Materials and methods

Experimental set-up

Each of the original 26 plates of the human miRIDIAN miRNA mimic library was split into two separate plates, denoted as "A" and "B" experiments, for the follow-up RNAi screening assays. All experiments were performed three times (i.e., A1, A2, A3 and B1, B2, B3, respectively).

FCM-based RNAi screening and miRNA transfection verification

The human melanoma cell line MelJuSo was cultured in Iscove's modified Dulbecco's medium (Sigma Aldrich, Burlington, MA, USA) substituted with 10% fetal calf serum, 200 mM glutamine (Sigma–Aldrich), 100 units/mL penicillin, and 10 μg/mL streptomycin (Sigma–Aldrich) at 37°C in 5% CO_2. The human miRIDIAN miRNA mimic library (19.0, CS-001030, Dharmacon GE Healthcare, Lafayette, CO, USA), containing 2048 different human miRNAs (50 nM), was used for the RNAi screening. Forty-eight miRNAs were excluded to reach equal sample sizes on all screening plates.

An siRNA against human class II MHC transactivator (*CIITA*), siRNA Hs_CIITA_2 (100 nM, Qiagen) was used as the positive control for downregulation of HLA-DR. Two miRIDIAN microRNA mimics, cel-miR-67 (50 nM, Dharmacon) and cel-miR-239b (50 nM, Dharmacon), with sequences based on *C. elegans* miRNAs, were used as negative controls.

Moreover, a Dy547-labeled miRNA hairpin inhibitor based on the *C. elegans* miRNA cel-miR-67 was used to monitor delivery (50 nM, Dharmacon). For the FCM-based high-throughput screening, MelJuSo cells were reverse transfected using DharmaFECT transfection reagent #1 (Dharmacon), with 5000 cells per well in 96-well plates.

For the miRNA transfection verification, a forward transfection was carried out independently, with up to 15,000 cells per well in 96-well plates. Overall, the transfection experiment was performed according to the manufacturer's instructions.

In brief, the cells were either seeded 1 day before (i.e., forward) or resuspended on the day of transfection (i.e., reverse). The transfection mixture containing miRNA/siRNA (50/100 nM final concentration) and 0.15% DharmaFECT1 (Dharmacon) was vortexed at ~~40~~ 250 rpm at room temperature for 20 min prior to transfection. Afterward, treatment cells were incubated at 37°C in 5% CO_2 for 72 h. For antibody staining before FCM, cell-surface HLA-DR was labeled with a monoclonal antibody against human HLA-DR (clone L243) using the DyLight-488nm antibody labeling kit (Thermo Fischer Scientific, 46402). For FCM experiments, the BD FACSArray bioanalyzer (Becton Dickinson) was used with the following settings: FSC (212), SSC (362), Dy488 (345). The acquired FCM data were analyzed with FlowJo (V7.6.5) software (FlowJo, LLC, Ashland, OR, USA). The MelJuSo single-cell population was gated and the median fluorescence intensities were computed for further statistical analyses.

Quantitative real-time PCR (*qPCR*)

To validate the effect of the miRNA transfection on the transcript of *HLA-DRA*, a forward transfection of all selected miRNA molecules and the positive/negative siRNA/miRNA controls (same concentrations as described above for FCM analysis) was conducted in 48-well plates with 25,000 cells per well. After treatment, cells were incubated at 37°C in 5% CO_2 for 48 h prior to mRNA analysis. For the *qPCR* analysis, total RNA was extracted using the High Pure RNA Isolation Kit according to the manufacturer's instructions (Roche, Rotkreuz, Switzerland). RNA quality and concentration were determined using a NanoDrop 2000 spectrophotometer (Thermo Scientific, Reinach, Switzerland). cDNAs were synthesized using the Transcriptor High Fidelity cDNA Synthesis Kit according to the manufacturer's instructions (Roche). *qPCR* was performed using the TaqMan Fast Advanced Master Mix (Thermo Fisher #4444556) in the LightCycler 480 instrument (Roche) following the user's manual, with the TaqMan Gene Expression Assay (Thermo Fisher #4351370) targeting three human genes *HLA-DRA, HLA-DRB1, CIITA* and two housekeeping genes *GAPDH* and hypoxanthine phosphoribosyl-transferase 1 (*HPRT1*) (Assay IDs: Hs00219575, Hs04192464, Hs00172106, Hs02758991, and Hs02800695, respectively) according to the manufacturer's recommended protocol. In addition, an identical cDNA template prepared from human MelJuSo cells was used throughout the assays as a *qPCR* calibrator. The 10 μL qPCR reaction mix consisted of 5 μL of TaqMan Fast Advanced Master Mix (2×), 0.5 μL of TaqMan Assay (20×), and cDNA template in nuclease-free water.

The PCR reaction cycle conditions used were: 50°C for 2 min, 95°C for 20 s, followed by 45 cycles of 95°C for 3 s, and 60°C for 30 s. The fluorescent signals were measured at the annealing or extension step. Standard curves were generated separately for the target gene and both reference genes using serial dilutions of the cDNA template. All *qPCR* reactions were performed in duplicate in 384-well plates. Data were processed using the LightCycler 480 system software version 1.5.0, and analyzed using the advanced relative quantification module (Roche).

Briefly, the relative level of each gene transcript was determined as the mean crossing point value and the ratio of the *HLA-DRA*, *HLA-DRB1*, or *CIITA* to the reference genes *GAPDH* and *HPRT1*. Each sample was compared with the same ratio in the standard sample (i.e., the calibrator). Thus, the relative quantification is calibrator normalized with efficiency correction and the result of the data analysis is expressed as a normalized ratio.

Statistical analysis

Quality assessment and z-scores

We performed a quality assessment of the RNAi HTS assays by computing a specific parameter—the so-called *Z'* factor—which is commonly used in similar cell-based RNAi HTS experiments [18, 19]. Briefly, the *Z'* factor is a screening window coefficient which is dimensionless, with simple statistical characteristics that can be readily applied to each conducted assay. In our RNAi HTS assays, cells transfected with siRNA Hs_CIITA_2 were used as the positive control group, while negative controls were made up of different treatment groups including untreated cells, cells treated with transfection reagent DharmaFECT, and cells transfected with cel-miR-67 or cel-miR-239b. To validate all conducted experiments for single assays, we computed all the *Z'* factors with different negative controls and only included assays with a *Z'* factor value higher than 0.5 for quality assurance. Twenty-five out of twenty-six plates were available for the computation of plate-based statistics including data normalization and transformation into z-scores.

To achieve a more biologically significant measure of the experimental effect, we followed a statistical method proposed by Boutros and colleagues which is intended for cell-based RNAi screening analysis [19]. We conducted plate-based MFI data normalization by dividing each MFI measurement by the plate-wise median MFI value. The robust z-scores were then derived via the following equation:

$$z_{kj} = \frac{y_{kj} - M}{\text{MAD}},$$

where M denotes the median of the normalized plate values and MAD corresponds to the Median Absolute Deviation of the normalized plate values. Note here that positive and negative control values are entirely omitted in the normalization procedure.

Hit identification and sensitivity analysis

We defined z-scores $+4$ and -3 as the thresholds for up- and downregulating miRNAs, respectively, for surface HLA-DR expression. The asymmetry in threshold definition accounts for the slightly skewed distribution of z-scores (see Supporting information Fig. S4), and the choice of threshold values balances the need for high (absolute) z-scores for possible hits as well as for achieving a sufficient sample size of possible hits.

A permutation approach was chosen for sensitivity analysis to assess the range of z-scores for 15 identified hits (see "Results"). For each identified hit, we replaced the normalized MFI values of randomly chosen samples with the normalized MFI values of that particular hit sample and recomputed the z-score. We repeated this procedure for all possible combinations, resulting in the distribution of z-scores for each hit. Both the location and width of such a z-score distribution give an indication of the robustness of the hit identification.

Statistical modeling of the FCM and qPCR

Sample size was N = 3 for FCM and N = 4 for qPCR. A linear mixed-effect model with a fixed effect was used for treatment (three levels: negative control, downward regulation, and upward regulation) and a random slope was used for each plate and each treatment, thus, accounting for the data structure of the experimental design. We transformed the outcome variable (MFI in the case of the verification experiment and the normalized ratio in case of qPCR) via ordered quantile normalization to ensure a normally distributed outcome in the linear mixed-effect model [55]. Estimated marginal means were employed to compute the contrasts of the two treatments and compare them with the negative control samples [56]. No p-value adjustment for multiple comparisons was used, as the p-values were exploratory rather than confirmatory in this study.

Statistical significance and software

A p-value <0.05 was considered statistically significant. All analyses were performed with R version 4.0.2 [57].

Acknowledgments: The authors would like to thank Jeannie Wurz for proofreading and editing the manuscript, Marcel Schiff, Lena Matthiss, Azam Jamaati, and Sibylle Rohrbach for their excellent technical support, Paul Kunath, Jaison Phour, and Christoph Mathieu for their help with different pilot experiments. The study was supported by an institutional grant from the Department of Anaesthesiology and Pain Medicine, Inselspital, Bern University Hospital, University of Bern, Bern, Switzerland (MY-YH, Gesuch Nr. HEYF-1-21).
Open access funding provided by Inselspital Universitatsspital Bern.

Conflict of interest: All authors declare that they have no financial or commercial conflict of interest.

Authors' contributions: Study concept and design: FS, MY-YH, CL. Acquisition of data: MS, MH (Houseman), LZ, CL, MY-YH. Analysis and interpretation of data: FS, MY-YH, CL, AH, MH (Houseman), MS, LZ, MH (Huber). Statistics: MH (Huber), MY-YH. Drafting the manuscript: MY-YH, MH (Houseman), MH (Huber). Revising and approval of the final version: all authors.

All authors agree to be accountable for all aspects of the work and ensure that questions related to the accuracy or integrity of any part of the work are appropriately investigated and resolved.

Data availability statement: The data that support the findings of this study are available from the corresponding author upon reasonable request.

Peer review: The peer review history for this article is available at https://publons.com/publon/10.1002/eji.202149735.

References

1 **Neefjes, J., Jongsma, M. L. M., Paul, P. and Bakke, O.**, Towards a systems understanding of MHC class I and MHC class II antigen presentation. *Nat. Rev. Immunol.* 2011. **11**: 823–836.

2 **Viallard, J. F., Bloch-Michel, C., Neau-Cransac, M., Taupin, J. L., Garrigue, S., Miossec, V., Mercie, P. et al.**, HLA-DR expression on lymphocyte subsets as a marker of disease activity in patients with systemic lupus erythematosus. *Clin. Exp. Immunol.* 2001. **125**: 485–491.

3 **Sáez-Cirión, A., Lacabaratz, C., Lambotte, O., Versmisse, P., Urrutia, A., Boufassa, F., Barré-Sinoussi, F., Delfraissy, J.-.F. et al.**, HIV controllers exhibit potent CD8 T cell capacity to suppress HIV infection ex vivo and peculiar cytotoxic T lymphocyte activation phenotype. *Proc. Natl. Acad. Sci. U. S. A.* 2007. **104**: 6776–6781.

4 **Saraiva, D. P., Jacinto, A., Borralho, P., Braga, S. and Cabral, M. G.**, HLA-DR in Cytotoxic T Lymphocytes Predicts Breast Cancer Patients' Response to Neoadjuvant Chemotherapy. *Front. Immunol.* 2018. **9**: 2605.

5 **Monneret, G., Lepape, A., Voirin, N., Bohé, J., Venet, F., Debard, A.-L., Thizy, H. et al.**, Persisting low monocyte human leukocyte antigen-DR expression predicts mortality in septic shock. *Intensive Care Med.* 2006. **32**: 1175–1183.

6 **Wakefield, C. H., Carey, P. D., Foulds, S., Monson, J. R. T. and Guillou, P. J.**, Changes in major histocompatibility complex class II expression in monocytes and T cells of patients developing infection after surgery. *Br. J. Surg.* 1993. **80**: 205–209.

7 **Venet, F., Tissot, S., Debard, A.-L., Faudot, C., Crampé, C., Pachot, A., Ayala, A. et al.**, Decreased monocyte human leukocyte antigen-DR expression after severe burn injury: Correlation with severity and secondary septic shock. *Crit. Care Med.* 2007. **35**: 1910–1917.

8 **Galbraith, N., Walker, S., Galandiuk, S., Gardner, S. and Polk, H. C.**, The Significance and Challenges of Monocyte Impairment: For the Ill Patient and the Surgeon. *Surg. Infect. (Larchmt)*. 2016. **17**: 303–312.

9 **Venet, F. and Monneret, G.**, Advances in the understanding and treatment of sepsis-induced immunosuppression. *Nat. Rev. Nephrol.* 2018. **14**: 121–137.

10 **Drewry, A. M., Ablordeppey, E. A., Murray, E. T., Beiter, E. R., Walton, A. H., Hall, M. W. and Hotchkiss, R. S.**, Comparison of monocyte human leukocyte antigen-DR expression and stimulated tumor necrosis factor alpha production as outcome predictors in severe sepsis: a prospective observational study. *Crit. Care*. 2016. **20**: 334.

11 **Cheadle, W. G., Hershman, M. J., Wellhausen, S. R. and Polk, H. C.**, HLA-DR antigen expression on peripheral blood monocytes correlates with surgical infection. *Am. J. Surg.* 1991. **161**: 639–645.

12 **Jeannet, R., Daix, T., Formento, R., Feuillard, J. and François, B.**, Severe COVID-19 is associated with deep and sustained multifaceted cellular immunosuppression. *Intensive Care Med.* 2020. **46**: 1769–1771.

13 **Spinetti, T., Hirzel, C., Fux, M., Walti, L. N., Schober, P., Stueber, F., Luedi, M. M. and Schefold, J. C.**, Reduced Monocytic Human Leukocyte Antigen-DR Expression Indicates Immunosuppression in Critically Ill COVID-19 Patients. *Anesth. Analg.* 2020. **131**: 993–999.

14 **Kox, M., Frenzel, T., Schouten, J., Van De Veerdonk, F. L., Koenen, H. J. P. M. and Pickkers, P.**, COVID-19 patients exhibit less pronounced immune suppression compared with bacterial septic shock patients. *Crit. Care*. 2020. **24**: 263.

15 **Monneret, G., Cour, M., Viel, S., Venet, F. and Argaud, L.**, Coronavirus disease 2019 as a particular sepsis: a 2-week follow-up of standard immunological parameters in critically ill patients. *Intensive Care Med.* 2020. **46**: 1764–1765.

16 **Paul, P., Van Den Hoorn, T., Jongsma, M. L. M., Bakker, M. J., Hengeveld, R., Janssen, L., Cresswell, P. et al.**, A Genome-wide multidimensional RNAi screen reveals pathways controlling MHC class II antigen presentation. *Cell*. 2011. **145**: 268–283.

17 **Wubbolts, R., Fernandez-Borja, M., Oomen, L., Verwoerd, D., Janssen, H., Calafat, J., Tulp, A. et al.**, Direct vesicular transport of MHC class II molecules from lysosomal structures to the cell surface. *J. Cell Biol.* 1996. **135**: 611–622.

18 **Zhang, J.-H., Chung, T. D.Y. and Oldenburg, K. R.**, A simple statistical parameter for use in evaluation and validation of high throughput screening assays. *J. Biomol. Screening*. 1999. **4**: 67–73.

19 **Boutros, M., Bras, L. P. and Huber, W.**, Analysis of cell-based RNAi screens. *Genome Biol.* 2006. **7**.

20 **Agrawal, S. and Kandimalla, E. R.**, Antisense and siRNA as agonists of Toll-like receptors. *Nat. Biot*. 2004. **22**: 1533–1537.

21 **Reynolds, A., Anderson, E. M., Vermeulen, A., Fedorov, Y., Robinson, K., Leake, D., Karpilow, J. et al.**, Induction of the interferon response by siRNA is cell type- and duplex length-dependent. *RNA*. 2006. **12**: 988–993.

22 **Steimle, V., Otten, L. A., Zufferey, M. and Mach, B.**, Complementation cloning of an MHC class II transactivator mutated in hereditary MHC class II deficiency (or bare lymphocyte syndrome). *Cell*. 1993. **75**: 135–146

23 **Accolla, R. S., Ramia, E., Tedeschi, A. and Forlani, G.**, CIITA-Driven MHC Class II Expressing Tumor Cells as Antigen Presenting Cell Performers: Toward the Construction of an Optimal Anti-tumor Vaccine. *Front. Immunol.* 2019. **10**.

24 **Denzin, L. K., Hammond, C. and Cresswell, P.**, HLA-DM interactions with intermediates in HLA-DR maturation and a role for HLA-DM in stabilizing empty HLA-DR molecules. *J. Exp. Med.* 1996. **184**: 2153–2166.

25 **Cajander, S., Tina, E., Bäckman, A., Magnuson, A., Strålin, K., Söderquist, B. and Källman, J. k.**, Expression of mRNA levels of HLA-DRA in relation to monocyte HLA-DR: a longitudinal sepsis study. *Critical Care*. 2015. **19**: P45.

26 **Lam, J. K. W., Chow, M. Y. T., Zhang, Y. and Leung, S. W. S.**, siRNA Versus miRNA as Therapeutics for Gene Silencing. *Molecular Therapy-Nucleic Acids*. 2015. **4**

27 **Filipowicz, W., Bhattacharyya, S. N. and Sonenberg, N.**, Mechanisms of post-transcriptional regulation by microRNAs: are the answers in sight? *Nat. Rev. Genet.* 2008. **9**: 102–114.

28 **Bartel, D. P.**, MicroRNAs: target recognition and regulatory functions. *Cell*. 2009. **136**: 215–233

29 **Braun, J. E., Huntzinger, E. and Izaurralde, E.**, A Molecular Link between miRISCs and Deadenylases Provides New Insight into the Mechanism of Gene Silencing by MicroRNAs. *Csh Perspect Biol*. 2012. **4**.

30 **Catalanotto, C., Cogoni, C. and Zardo, G.**, MicroRNA in Control of Gene Expression: An Overview of Nuclear Functions. *Int. J. Mol. Sci.* 2016. 1712, **17**.

31 **Lewis, B. P., Shih, I.-H., Jones-Rhoades, M. W., Bartel, D. P. and Burge, C. B.**, Prediction of mammalian microRNA targets. *Cell*. 2003. **115**: 787–798

32 **Carroll, A. P., Tran, N., Tooney, P. A. and Cairns, M., J.** Alternative mRNA fates identified in microRNA-associated transcriptome analysis. *BMC Genomics*. 2012. **13**: 561

33 **Betel, D., Koppal, A., Agius, P., Sander, C. and Leslie, C.**, Comprehensive modeling of microRNA targets predicts functional non-conserved and non-canonical sites. *Genome Biol.* 2010. **11**: R90

34 **Agarwal, V., Bell, G. W., Nam, J-Wu and Bartel, D. P.**, Predicting effective microRNA target sites in mammalian mRNAs. *Elife*. 2015. **4**.

35 **Mcgeary, S. E., Lin, K. S., Shi, C. Y., Pham, T. M., Bisaria, N., Kelley, G. M. and Bartel, D. P.**, The biochemical basis of microRNA targeting efficacy. *Science*. 2019. **366**: 1470-+.

36 **Chen, Y. and Wang, X.**, miRDB: an online database for prediction of functional microRNA targets. *Nucleic. Acids. Res.* 2020. **48**: D127–D131.

37 **Liu, W. and Wang, X.**, Prediction of functional microRNA targets by integrative modeling of microRNA binding and target expression data. *Genome Biol.* 2019. **20**: 18.

38 **Hensler, T., Hecker, H., Heeg, K., Heidecke, C. D., Bartels, H., Barthlen, W., Wagner, H., Siewert, J. R. et al.**, Distinct mechanisms of immunosuppression as a consequence of major surgery. *Infection and Immunity*. 1997. **65**: 2283–2291.

39 **Erdoes, G., Lippuner, C., Kocsis, I., Schiff, M., Stucki, M., Carrel, T., Windecker, S., Eberle, B., Stueber, F. and Book, M.**, Technical Approach Determines Inflammatory Response after Surgical and Transcatheter Aortic Valve Replacement. *PLoS One*. 2015. **10**: e0143089.

40 **Menges, P., Kessler, W., Kloecker, C., Feuerherd, M., Gaubert, S., Diedrich, S., Van Der Linde, J. et al.**, Surgical Trauma and Postoperative Immune Dysfunction. *European Surgical Research*. 2012. **48**: 180–186.

41 **Satoh, A., Miura, T., Satoh, K., Masamune, A., Yamagiwa, T., Sakai, Y., Shibuya, K. et al.**, Human leukocyte antigen-DR expression on peripheral monocytes as a predictive marker of sepsis during acute pancreatitis. *Pancreas*. 2002. **25**: 245–250.

42 **Haveman, J., Van Den Berg, A. P., Verhoeven, E. L., Nijsten, M. W., Van Den Dungen, J. J., The, T. H. and Zwaveling, J.**, HLA-DR expression on monocytes and systemic inflammation in patients with ruptured abdominal aortic aneurysms. *Critical Care*. 2006. **10**: R119.

43 **Franke, A., Lante, W., Zoeller, L. G., Kurig, E., Weinhold, C. and Markewitz, A.**, Delayed recovery of human leukocyte antigen-DR expression after cardiac surgery with early non-lethal postoperative complications: only an epiphenomenon? *Interact Cardiovasc Thorac Surg*. 2008. **7**: 207–211.

44 **Diener, C., Keller, A. and Meese, E.**, Emerging concepts of miRNA therapeutics: from cells to clinic. *Trends Genet.* 2022. 613–626.

45 **Chakraborty, C., Sharma, A. R., Sharma, G. and Lee, S.-S.**, Therapeutic advances of miRNAs: A preclinical and clinical update. *J. Adv. Res.* 2021. **28**: 127–138.

46 **Peng, Y. and Croce, C. M.**, The role of MicroRNAs in human cancer. *Signal Transduct Tar*. 2016. **1**.

47 **Zuckerman, J. E. and Davis, M. E.**, Clinical experiences with systemically administered siRNA-based therapeutics in cancer. *Nat. Rev. Drug. Discov.* 2015. **14**: 843–856.

48 **Mahmoodi Chalbatani, G., Dana, H., Gharagouzloo, E., Grijalvo, S., Eritja, R., Logsdon, C. D., Memari, F. et al.**, Small interfering RNAs (siRNAs) in cancer therapy: a nano-based approach. *Int. J. Nanomed.* 2019. **14**: 3111–3128.

49 **Essandoh, K. and Fan, G.-C.**, Role of extracellular and intracellular microRNAs in sepsis. *Bba-Mol Basis Dis*. 2014. **1842**: 2155–2162.

50 **Szilagyi, B., Fejes, Z., Pocsi, M., Kappelmayer, J. and Nagy B., Jr.**, Role of sepsis modulated circulating microRNAs. *EJIFCC*. 2019. **30**: 128–145

51 **Wang, H., Zhang, P., Chen, W., Feng, D., Jia, Y. and Xie, L.**, Serum microRNA signatures identified by Solexa sequencing predict sepsis patients' mortality: a prospective observational study. *PLoS One*. 2012. **7**: e38885.

52 **Stickel, N., Hanke, K., Marschner, D., Prinz, G., Köhler, M., Melchinger, W., Pfeifer, D. et al.**, MicroRNA-146a reduces MHC-II expression via targeting JAK/STAT signaling in dendritic cells after stem cell transplantation. *Leukemia*. 2017. **31**: 2732–2741.

53 **Cazalis, M.-A., Friggeri, A., Cavé, L., Demaret, J., Barbalat, V., Cerrato, E., Lepape, A. et al.**, Decreased HLA-DR antigen-associated invariant chain (CD74) mRNA expression predicts mortality after septic shock. *Crit. Care*. 2013. **17**: R287.

54 **Codolo, G., Toffoletto, M., Chemello, F., Coletta, S., Soler Teixidor, G., Battaggia, G., Munari, G. et al.**, Helicobacter pylori Dampens HLA-II Expression on Macrophages via the Up-Regulation of miRNAs Targeting CIITA. *Front. Immunol.* 2020. **10**.

55 **Peterson, R. A. and Cavanaugh, J. E.**, Ordered quantile normalization: a semiparametric transformation built for the cross-validation era. *J. Appl. Stat.* 2020. **47**: 2312–2327.

56 emmeans: Estimated Marginal Means, aka Least-Squares Means. R package version 1.6.0. (2021).

57 R: A language and environment for statistical computing. *R Foundation for Statistical Computing*, Vienna, Austria. 2020.

Abbreviations: **miRNA:** microRNA · **RNAi:** ribonucleic acid interference · **FCM:** flow cytometry · **qPCR:** quantitative real-time PCR

Full correspondence:: Dr. Melody Ying-Yu Huang and Frank Stüber, Universitätsklinik für Anästhesiologie und Schmerztherapie, Inselspital, 3010, Bern, Switzerland.
e-mail: melody.yingyu.huang@gmail.com; frank.stueber@insel.ch

Received: 24/11/2021
Revised: 15/4/2022
Accepted: 23/5/2022
Accepted article online: 25/5/2022